Molecular Crystals and Liquid Crystals

Publication details, including instructions for authors and subscription information:
http://www.tandfonline.com/loi/gmcl20

Organic Superconductors

Gunzi Saito [a] & Mitsuhiko Maesato [a]

[a] Department of Chemistry, Graduate School of Science, Kyoto University, Kitashirakawa, Sakyo-ku, Kyoto, Japan

Version of record first published: 31 Jan 2007

To cite this article: Gunzi Saito & Mitsuhiko Maesato (2006): Organic Superconductors, Molecular Crystals and Liquid Crystals, 455:1, 31-46

To link to this article: http://dx.doi.org/10.1080/15421400600803655

Mol. Cryst. Liq. Cryst., Vol. 455, pp. 31–46, 2006

ISSN: 1542-1406 print/1563-5287 online
DOI: 10.1080/15421400600803655

Taylor & Francis
Taylor & Francis Group

Organic Superconductors

Gunzi Saito
Mitsuhiko Maesato
Department of Chemistry, Graduate School of Science,
Kyoto University, Kitashirakawa, Sakyo-ku, Kyoto, Japan

We briefly describe the strategies to increase (or decrease) the electronic dimensionality to suppress (or induce) metal-insulator transition and discuss the structural and physical properties, ground state and phase diagram of TMTSF and ET superconductors. Then we touch on the other superconductors including single component ones and unidentified superconducting organics (USO) reported so far.

Keywords: ET; organic superconductors; spin-liquid state; uni-axial strain; unidentified superconducting organics (USO)

1. STRATEGY TO MODIFY ELECTRONIC DIMENSIONALITY

Since the metallic state in the one-dimensional (1D) electronic system is unstable, an increase in the electronic dimensionality is necessary to prevent the nesting of Fermi surfaces. Several attempts have been made through "pressure," "heavy atom substitution" or "peripheral addition of alkylchalcogeno groups" (Fig. 1) [1,2]. The HMTTeF molecules afforded stable metallic phase without any trace of superconductivity [3]. The BO molecules also afforded stable 2D metals owing to the strong self-asembling ability [4]. To destabilize the metallic state of the BO complexes, the substitution of one ethylenedioxy group with ethylenedithio group (BO → EOET) or the elimination of one ethylenedioxy group (BO → EDO) was examined. They are found to be very efficient to provide charge localized phases or metal-insulator (MI) transitions [5,6]. Several superconductor (SC)s have been prepared based on TMTSF, ET, BO and a variety of analogues of EOET and

Address correspondence to Gunzi Saito, Department of Chemistry, Graduate School of Science, Kyoto University, Kitashirakawa, Sakyo-ku, Kyoto, 606-8502, Japan. E-mail: saito@kuchem.kyoto-u.ac.jp

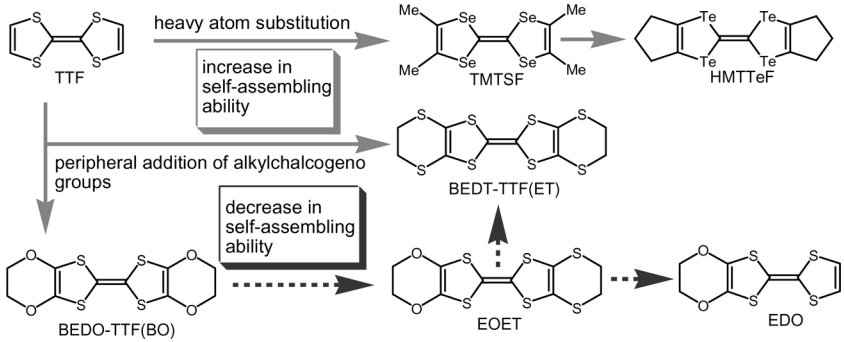

FIGURE 1 Strategy for chemical modification of the TTF molecule to increase (arrows) or decrease (dotted arrows) the electronic dimensionality by the aid of enhance or suppress the self-assembling ability of the donor molecules, respectively.

EDO, though EOET and EDO themselves did not afford SCs (see Section 10).

2. TMTSF AND TMTTF 1D SUPERCONDUCTORS

The most successful molecule by "heavy atom substitution" is TMTSF, which has provided eight quasi-1D SCs; $(TMTSF)_2X$ ($X = PF_6$, AsF_6, SbF_6, NbF_6, TaF_6, ClO_4, ReO_4 and FSO_3) with $T_c < 3$ K [2,7–9]. Among them the NbF_6 salt was recently prepared using room-temperature ionic liquid (1-ethyl-3-methyl-imidazolium)NbF_6 as electrolyte [9]. $(TMTSF)_2NbF_6$ is isostructural to other $(TMTSF)_2X$. The MI transition at 12 K at ambient pressure (AP) due to spin density wave (SDW) was suppressed under pressure and a superconductivity appeared with on-set superconducting transition tempetature (T_c) of 1.26 K (mid-point $T_c = 1.12$ K) at 1.2 GPa [9]. The isomorphous $(TMTTF)_2X$ salts displayed superconductivity under high pressure with T_c less than 2 K for $X = Br$ [10], PF_6 [11], and BF_4 [12]. $(TMTSF)_2ClO_4$ is the only AP SC among them and did not show the Hebel-Slichter coherence peak indicating non *s*-wave type SC [13]. A generalized phase diagram including $(TMTTF)_2X$ and $(TMTSF)_2X$ indicates that the superconducting phase neighbors the magnetic SDW phase [14].

3. ET AND BO 2D SUPERCONDUCTORS

The "peripheral addition of alkylchalcogeno groups" to a parent molecule TTF has successfully produced 2D BO [4] and ET [1,15]

conductors. The robust intermolecular interactions in the BO complexes have provided a metallic state even in the strongly disordered systems. The BO complexes hardly exhibited any phase transition including the superconducting one (only two SCs ($T_c \leq 1.5$ K) were found) [16,17].

As for ET compounds, different kinds of ET••ET (π–π, S••S) and ET••anion (hydrogen bonds) intermolecular interactions, large conformational freedom of ethylene groups, flexible molecular framework, fairly narrow bandwidth and strong electron correlations gave a rich variety of complexes with different crystal and electronic structures ranging from insulators to SCs. About 60 ET SCs are so far known. Currently β'-$(ET)_2ICl_2$ (on-set $T_c = 14.2$ K and midpoint $T_c = 13.4$ K at 8.2 GPa [18]) and κ-$(d_8$-$ET)_2Cu[N(CN)_2]Cl$ ($T_c = 13.1$ K at 0.03 GPa) [19] show the highest values of T_c under pressures, while both are Mott insulators at AP. At AP, κ-$(d_8$-$ET)_2Cu(CN)[N(CN)_2]$ shows the highest T_c of 12.3 K [20] followed by κ-$(h_8$-$ET)_2Cu[N(CN)_2]Br$ ($T_c = 11.8$ K) [21].

4. κ-TYPE 10 K CLASS SUPERCONDUCTORS

The four κ-type SCs κ-$(ET)_2X$ {X = $Cu(NCS)_2$, $Cu[N(CN)_2]Cl$, $Cu[N(CN)_2]Br$ and $Cu(CN)[N(CN)_2]$} share some common structural and physical properties. Figure 2 shows the crystal structure of the

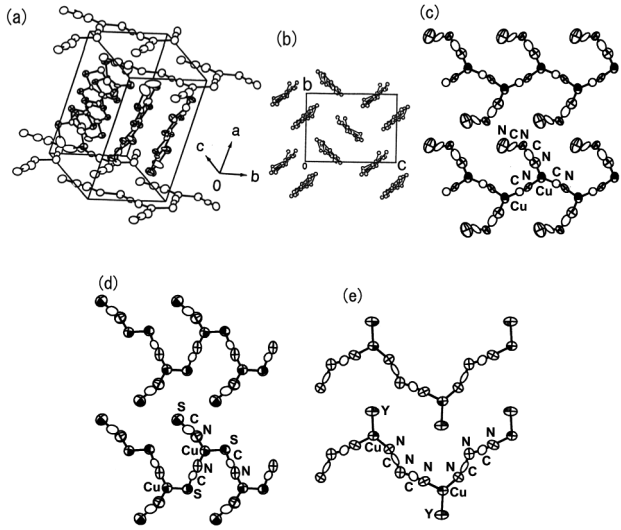

FIGURE 2 (a) Crystal structure of κ-$(ET)_2Cu(NCS)_2$. (b) Packing of ET molecules viewed along the long molecular axis. Anion structures of κ-$(ET)_2X$, X = $Cu(CN)[N(CN)_2]$ (c), $Cu(NCS)_2$ (d), $Cu[N(CN)_2]Y$ (Y = Cl, Br) (e).

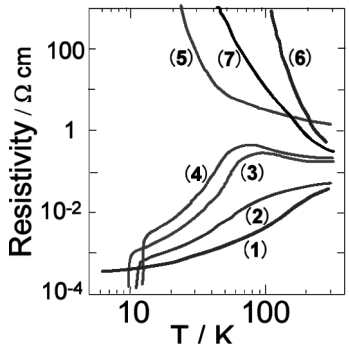

FIGURE 3 Temperature dependences of resistivity of 10 K class superconductors κ-$(ET)_2X$ (X = Cu(CN)[N(CN)$_2$] (**2**), Cu(NCS)$_2$ (**3**), Cu[N(CN)$_2$]Br (**4**), Cu[N(CN)$_2$]Cl (**5**)) are compared with those of a good metal with low T_c β-$(ET)_2AuI_2$ (**1**), strongly electron correlated insulator θ-$(ET)_2Cu_2(CN)[N(CN)_2]_2$ (**6**) and a Mott insulator κ-$(ET)_2Cu_2(CN)_3$ (**7**) at AP. (See COLOR PLATE I)

prototype Cu(NCS)$_2$ salt [22] and anion structures of κ-$(ET)_2X$. Although these ET salts have similar structural aspects, their transport properties differ apparently (Fig. 3). The Cu(CN)[N(CN)$_2$] salt (**2**) showed a monotonous decrease of resistivity with upper curvature down to T_c. The Cu[N(CN)$_2$]Br salt (**4**) exhibited a similar behavior to that of the Cu(NCS)$_2$ salt (**3**) without a metallic regime near RT. The Cu[N(CN)$_2$]Cl salt (**5**) showed a semiconductor ($\varepsilon_g = 24$ meV)–semiconductor ($\varepsilon_g = 104$ meV) transition at *ca*. 42 K due to an antiferromagnetic (AF) fluctuation [23] resulting in a weak ferromagnet below 22 K. Under a weak pressure, it showed a similar temperature dependence to that of the Cu[N(CN)$_2$]Br salt.

The Cu[N(CN)$_2$]Cl salt showed a complicated *T*-*P* phase diagram (Fig. 4a) [24,25]; a non-metallic phase (N1) down to 60 K, low-D AF fluctuation (N2) down to 30–35 K, 3D AF ordered phase (N3) and weak ferromagnet (N4) below 22 K. Weak ferromagnetic and superconducting phases coexist below 13 K (incomplete superconducting phase; I-SC-2). Another I-SC phase (I-SC-1) appeared at *ca*. 20–30 MPa then the complete superconducting (C-SC) phase followed at higher pressures. Below these superconducting phases, reentrant nonmetallic (RN) phase resides. Similar *T*-*P* phase diagrams were obtained for κ-$(d_8\text{-}ET)_2$ Cu[N(CN)$_2$]Y (Y = Cl, Br) with a parallel shift of pressure [27].

5. SUPERCONDUCTING CHARACTERISTICS

The Cu(NCS)$_2$ salt gave higher H_{c2} values in the 2D plane than H_{Pauli} [28]. No Hebel-Slichter coherence peak was observed in both Cu(NCS)$_2$

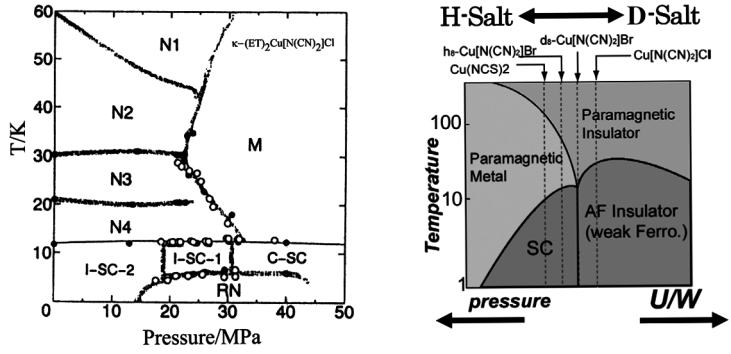

(a) (b)

FIGURE 4 Pressure-temperature phase diagram of (a) κ-(h_8-ET)$_2$Cu[N(CN)$_2$]Cl [24,25] (**M**: metallic phase). (b) Simplified phase diagram for κ-(ET)$_2$X [26]. Geometrical isotope effect is represented by arrow above the figure. The diagram cannot include both κ-(ET)$_2$Cu$_2$(CN)$_3$, which does not exhibit AF state and κ-(ET)$_2$Cu(CN)[N(CN)$_2$], which does not exhibit paramagnetic non-metallic phase although T_c is higher than 11 K.

and Cu[N(CN)$_2$]Br salts [29] in ^{1}H-NMR measurements, ruling out the BCS *s*-wave state. The symmetry of the superconducting state of the Cu(NCS)$_2$ salt has been controversially described as normal BCS-type or non-BCS type. Scanning tunneling spectroscopy showed the *d*-wave symmetry with line nodes [30], and thermal conductivity measurements showed that the symmetry is of d_{xy} [31]. Inverse isotope effect has so far been observed for the Cu(NCS)$_2$ [30], Cu(CN)[N(CN)$_2$] [20] and Cu[N(CN)$_2$]Cl [19] salts, and normal isotope effect for the Cu[N(CN)$_2$]Br salt [32].

A *T*-*P* phase diagram for κ-(ET)$_2$X (Fig. 4b) has been proposed which includes the Cu(NCS)$_2$, Cu[N(CN)$_2$]Br and Cu[N(CN)$_2$]Cl salts [26]. This diagram is a simplified one compared with the experimentally observed one (Fig. 4a), but is very convenient and useful to explain the general trends for these salts. The phase diagram and "geometrical isotope effect" [33] point out that T_c decreases with increasing pressure if only the parameter U/W or density of states at Fermi level $D(\varepsilon_F)$ is taken into account. This tendency has been observed under hydrostatic pressure but not under uniaxial pressure (see Section 7).

6. CONTROL OF U/W AND BAND FILLING: κ'-(ET)$_2$Cu$_2$(CN)$_3$

A Mott insulator κ-(ET)$_2$Cu$_2$(CN)$_3$ (**7** in Fig. 3) was converted to a metal and SC by applying hydrostatic pressure of 0.35 GPa with

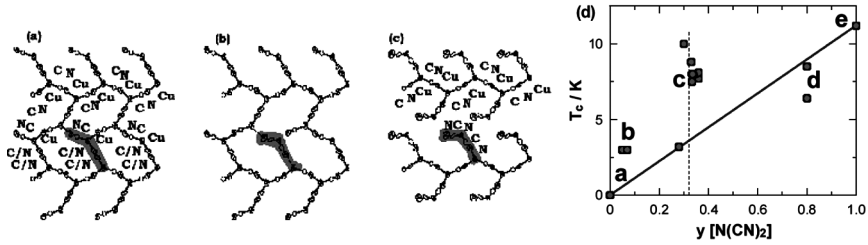

FIGURE 5 The anion structures of (a) κ-$(ET)_2Cu_2(CN)_3$ and (c) κ-$(ET)_2Cu(CN)[N(CN)_2]$. (b) A schematic figure of κ'-$(ET)_2(Cu^{1+})_{2-x-y}(Cu^{2+})_x(CN)_{3-2y}[N(CN)_2]_y$ with $y \sim 0.1$ [35]. (d) Relation between the content of $N(CN)_2$, y and T_c in several crystals of κ' salt: κ-$(ET)_2(Cu^{1+})_{2-x-y}(Cu^{2+})_x(CN)_{3-2y}[N(CN)_2]_y$. As for points **a**–**e**, see text. Dashed line indicates the samples of $y \approx 0.3$.

on-set T_c of 3.9 K through a Mott insulator-metal transition at 13–14 K with a resistivity drop by 10^5 [34]. On the other hand, an isostructural salt κ'-$(ET)_2Cu_2(CN)_3$, which contained a small amount of Cu^{2+}, exhibited a metal-SC transition without Mott insulating state [34]. Later, it was found that exact chemical formula of κ'-$(ET)_2Cu(CN)_3$ was κ-$(ET)_2(Cu^{1+}_{2-x-y}Cu^{2+}_x)\{(CN)_{3-2y}[N(CN)_2]_y\}$ and its transport natures were governed by the content of Cu^{2+} (x) and ligand $[NC\text{-}N\text{-}CN]^{1-}$ (y) [35]. Owing to the very similar shape, size and equal charge between $[Cu(CN)_2]$ and $[N(CN)_2]$, they were replaceable to each other in the anion layer (Figs. 5a–c). At $x = 0$ and $y = 0$, the salt is a Mott insulator $X = Cu_2(CN)_3$ (point **a** in Fig. 5d), while the other extreme side ($x = 0$, $y = 1$) is a SC $X = Cu(CN)[N(CN)_2]$ with $T_c = 11.2$ K at AP (point **e**). By changing both x (80–1200 ppm) and y (preferential values of y are 0.05 (point **b**), 0.3–0.4 (**c**), 0.8 (**d**)), the T_c was tuned from 3 to 11 K. At $y = 0.3$–0.4, the T_c covered from 3 to 10 K and the crystals with different T_c had different x values indicating that the charge of ET was modified from +0.5 to $+0.5(1 - x)$, that corresponds to the change of chemical potential. T_c increased with increasing x (= the content of Cu^{2+}) up to 400 ppm and then T_c decreased.

7. HYDROSTATIC-PRESSURE VS. UNIAXIAL-STRAIN

In general, T_c decreased rapidly with increasing hydrostatic pressure ($dT_c/dP = -(30\text{–}35)\,K\,GPa^{-1}$ for the $Cu(NCS)_2$ salt [36] and $-24\,K\,GPa^{-1}$ for the $Cu[N(CN)_2]Br$ salt [37] except some special cases, κ-$(ET)_2Hg_{2.89}Br_8$ ($dT_c/dP \approx +13\,K\,GPa^{-1}$) [38] and the $Cu[N(CN)_2]Cl$ salt (T_c increased at low pressure range then was suppressed at higher pressures $dT_c/dP = -34\,K\,GPa^{-1}$) [19]. The suppression rates of T_c by

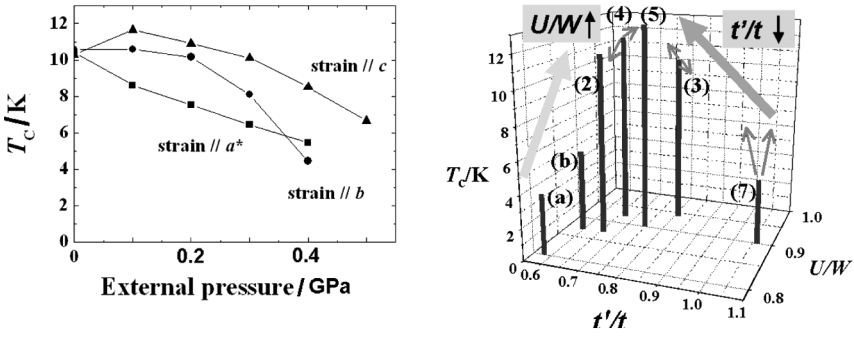

(a) (b)

FIGURE 6 (a) Pressure dependence of T_c of κ-$(ET)_2Cu(NCS)_2$ under uniaxial strain [44]. (b) T_c of κ-$(ET)_2X$ salts are plotted as function of t'/t and U/W [45]. X = I_3(a), $Ag(CN)_2{\cdot}H_2O$ (b), Cu(CN)[$N(CN)_2$] (**2**), $Cu(NCS)_2$ (**3**), Cu[$N(CN)_2$]Br (**4**), Cu[$N(CN)_2$]Cl (**5**) $Cu_2(CN)_3$ (**7**). Blue and yellow arrows indicate the direction of t'/t decreases and U/W increases, respectively. Red arrows correspond to the changes of T_c by applying uniaxial strain. (See COLOR PLATE II)

pressure for the 10 K class SCs are remarkably high compared to other SCs ($dT_c/dP = -1.0\,K\,GPa^{-1}$ for $(TMTSF)_2ClO_4$ [39] and $-7.8\,K\,GPa^{-1}$ for K_3C_{60} [40]). The hydrostatic pressure method, however, has a marked disadvantage that it does not provide direct information concerning about the anisotropy of the anisotropic organic conductors.

Early works on κ-$(ET)_2Cu(NCS)_2$ have been done by 1) tensile stress [41], 2) direct uniaxial compressive stress [42], and 3) uniaxial compressive stress using epoxy-method [43]. These involve so-called Poisson's effect. In general T_c decreased. An increase in T_c was only observed by 1 ($\Delta T_c = 0.6 \pm 0.5\,K$, $//b$). Later, several groups studied the uniaxial strain effects on T_c using epoxy-method without the Poisson's effect [44]. The uniaxial strain along the c-axis increased T_c with $dT_c/dP_c = \sim +13\,K\,GPa^{-1}$ up to 0.1 GPa (on-set $T_c = 11.2 \pm 0.4\,K$) followed by a decrease with $dT_c/dP_c \sim -12\,K\,GPa^{-1}$ (Fig. 6a) [44 (b)]. On the other hand, along the b-axis T_c is nearly constant up to 0.2 GPa and then decreased rapidly ($dT_c/dP_c \sim -28\,K\,GPa^{-1}$). Along the interlayer direction ($//a^*$), T_c decreased monotonically ($dT_c/dP_c \sim -(11\text{–}17)\,K\,GPa^{-1}$).

Figure 6b demonstrates the T_c of several κ-$(ET)_2X$ SCs with respect to the two parameters U/W and t'/t, where the latter represents the electronic anisotropy (Figs. 7a, b). The uniaxial strain experiments in Fig. 6b clearly revealed that the T_c increased as the U/W approaches unity and as the t'/t departs from unity (see Section 9) [45].

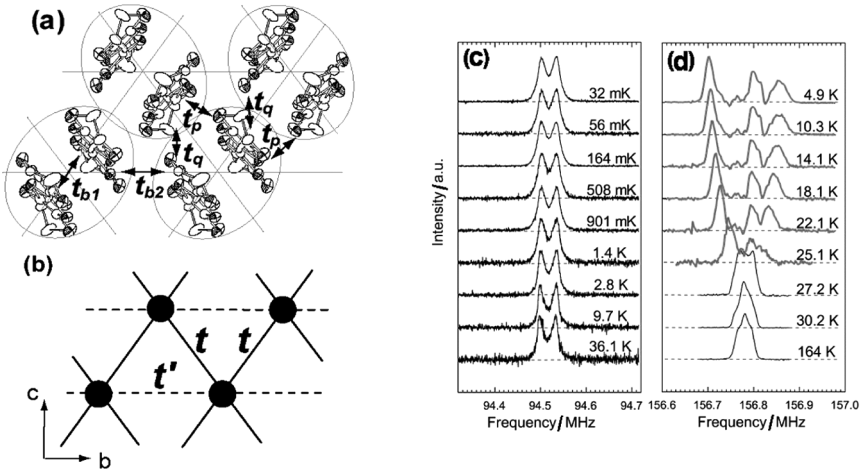

FIGURE 7 (a) Donor packing pattern of κ-$(ET)_2Cu_2(CN)_3$ along the a-axis (transfer integrals; $t_{b1} = 22\,meV$, $t_{b2} = 12\,meV$, $t_p = 8\,meV$ and $t_q = 3\,meV$) and (b) triangular spin lattice ($t'/t = 1.06$; $t' = t_{b2}$, $t = (|t_p| + |t_q|)/2$) composed of the ET dimer which is encircled by an ellipsoid in (a) and represented by closed circle in (b). Line shape of ^{1}H-NMR of (c) κ-$(ET)_2Cu_2(CN)_3$ [48] and (d) κ-$(ET)_2Cu[N(CN)_2]Cl$ [26].

8. TRIANGULAR SPIN LATTICE AND SPIN LIQUID STATE

Figure 3 compares the resistivity of three κ-type SCs (**2**–**4**) with those of κ-type Mott insulators (**5** and **7**), strongly electron correlated insulator θ-$(ET)_2Cu_2(CN)[N(CN)_2]_2$ (**6**) and a good metal having low T_c, β-$(ET)_2AuI_2$(**1**). κ-$(ET)_2Cu_2(CN)_3$ (**7**) showed a comparable σ_{RT} value to those of **2**–**6**. The energy gap ε_g of **7** (0.10–0.12 eV) is 4–5 times that of **5** (0.024 eV) and a half of that of **6** (0.17–0.19 eV). The semiconductive region of **3**–**6**, which is called as paramagnetic non-metallic phase in Figure 4b, is postulated to be a Mott insulating state. However the enhancement in the magnetic susceptibility due to the electron correlation is not significant compared to those of the typical Mott insulators (Table 1). The magnetic susceptibility, optical, thermopower and other measurements confirmed that the semiconductive-like region of **3** and **4** is neither the typical Mott insulator nor typical metal. The origin of the regime is still controversial, but the strong electron correlation is the most plausible cause. Figure 3 and the χ_{RT} in Table 1 show that the electron correlation increases in the order of **1** < **2** < **3** < **4** < **5** < **7** < **6**.

It has been generally observed that the superconducting state is located in close proximity to the magnetic-ordered state in cuprate,

TABLE 1 Characteristic Properties of ET Salts **1–7** and Others

	Conductivity σ_{RT} (ε_g)/ S cm^{-1}(eV)	χ_{RT} EPR,[1] static[2]/ 10^{-4} emu mol^{-1}	W_U, $W_U/\Delta E_d$[3]	t'/t[4]	Ground state at ambient pressure
I. Good metal					
κ-$(ET)_2I_3$	30	No data	0.61, 1.24	0.58	SC
β-$(ET)_2I_3$	60	4.6	0.59, 1.23	–	SC
β-$(ET)_2AuI_2$ **1**	20–60	3.4	0.57, 1.14	–	SC
II. 10 K class superconductor					
κ-$(ET)_2Cu(CN)[N(CN)_2]$ **2**	5–50	4.6	0.52, 1.16	0.66–0.71	SC
κ-$(ET)_2Cu(NCS)_2$ **3**	5–40	4.5–4.6, 4.4–4.5	0.57, 1.24	0.82–0.86	SC
κ-$(ET)_2Cu[N(CN)_2]Br$ **4**	5–50	4.5–5.5, 4.4–4.5	0.55, 1.12	0.68	SC
κ-$(ET)_2Cu[N(CN)_2]Cl$ **5**	2 (0.024 > 42 K)	4.5, 4.5–4.6	0.56, 1.10	0.75	AF
κ-$(ET)_2Cu_2(CN)_3$ **7**	2–7 (0.10 > 100 K)	5.5, 4.7	0.50, 1.11	1.06	
θ-$(ET)_2Cu_2(CN)[N(CN)_2]_2$ **6**	2–16 (0.16–0.20)	9.3, 10		–	CO
III. Mott insulator					
ET-TCNQ	10	8.8	0.41, 0.89	–	AF
β'-$(ET)_2ICl_2$	3×10^{-2}	9.6	0.27, 0.49	–	AF
β'-$(ET)_2AuCl_2$	10^{-1}–10^{-2}	9.6	0.25, 0.47	–	AF

[1]Measured in our group except β-$(ET)_2AuI_2$.

[2]Measured by K. Kanoda for salt **5** [26].

[3]$W_U/\Delta E_d$ is a ratio of the upper bandwidth (W_U = 0.50–0.57 eV) to dimerization energy (ΔE_d = 0.45–0.51 eV), which is a measure of W/U_{eff}. The calculated W of salt **7** (not dimerized ET system) is 0.65 eV.

[4]As for transfer integrals t and t', see Figure 7.

C_{60}, TMTSF and ET systems (SDW or AF state). However, the ground state of **7** differs from them distinctly. Figure 7a shows the donor packing of **7** where an ET dimer is a unit with $S = 1/2$ spin to form the triangular lattice with two kinds of transfer integrals $t = (|t_p|+|t_q|)/2$ and $t' = t_{b2}/2$ (Fig. 7b) [46,47]. Figures 7c,d compare the line shape of ^{1}H-NMR absorption of **7** and **5**. The latter salt exhibited a drastic change below 27 K owing to the formation of 3D AF ordering. On the other hand, the absorption band of **7** remains almost invariant down to 32 mK indicating non-spin-ordered (spin-liquid: SL) state [48]. The appearance of SL state in **7** can be explained in terms of the spin geometry of κ-$(ET)_2X$ which forms an anisotropic triangular lattice with varied t'/t (Table 1). Although the Mott insulators **5** and deuterated **4** have nearly the same W/U_{eff} as that of **7** (Fig. 6b), the less frustrated spins in **5** ($t'/t \sim 0.75$) and D-salt of **4** ($t'/t = 0.68$ for the H-salt) can lead to an AF ordered state. On the other hand, since the spin frustration is much significant in **7** ($t'/t = 1.06$), the formation of the AF state is suppressed at AP. Then the salt **7** forms the unprecedented SL state, which can be placed in Figure 4b by adding another axis t'/t besides U/W.

9. SUPERCONDUCTING STATE NEIGHBORING TO SL STATE

Figure 8 shows the temperature dependence of resistance of κ-$(ET)_2Cu_2(CN)_3$ under the uniaxial strain along the *b*-and *c*-axes. Along the *b*-axis, the semiconductor-like region remained clearly even at 0.5 GPa, while along the *c*-axis, the semiconductor-like region disappeared at 0.5 GPa. The uniaxial strains along the *b*- and *c*-axes

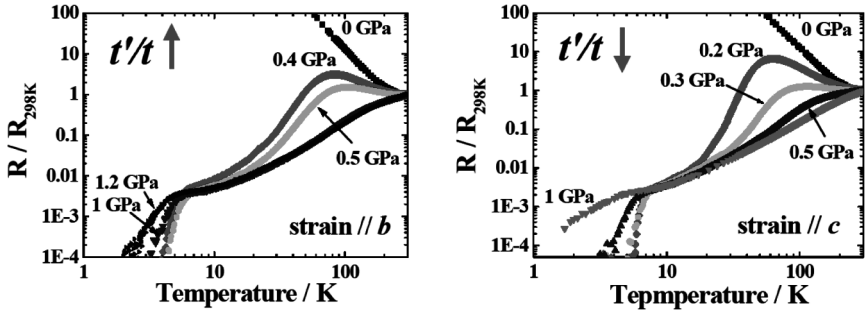

FIGURE 8 Temperature dependence of resistance of κ-$(ET)_2Cu_2(CN)_3$ by uni-axial strain epoxy-method along the *b*- (left) and *c*-axes (right). (See COLOR PLATE III)

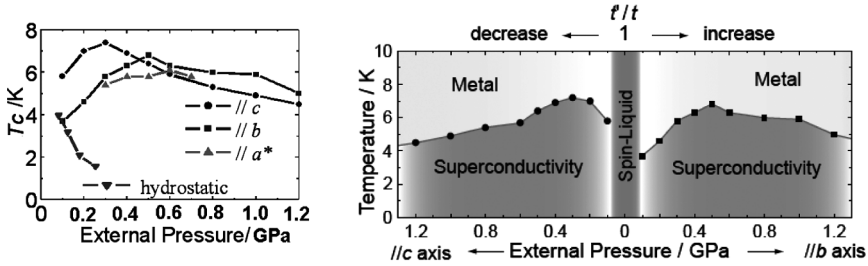

FIGURE 9 (a) Pressure dependence of on-set T_c of κ-$(ET)_2Cu_2(CN)_3$ by the uni-axial strain and hydrostatic pressure methods. (b) Temperature-uniaxial pressure phase diagram in the low temperature region.

resulted in the increase and decrease of t'/t, respectively. In both cases, a superconducting state readily appeared since the t'/t deviates from unity besides the increase of W/U_{eff}. It is noteworthy that the disappearance of the semiconductor-like region, appearance of the superconducting state and its T_c's are fairly anisotropic as shown in Figure 9. Compared to the hydrostatic results, the uniaxial method afforded 1) a much higher T_c value, 2) an increase of T_c at the initial pressure region, and 3) an anisotropic pressure dependence. Within the *bc*-plane, the superconducting state appeared above 0.1 GPa ($T_c = 3.8$ K ($//b$), 5.8 K ($//c$)) and T_c increased up to 6.8 K ($//b$, 0.5 GPa) and 7.2 K ($//c$, 0.3 GPa). Along the a^*-axis, the superconducting state appeared above 0.3 GPa.

A *T*-*P* phase diagram for κ-$(ET)_2Cu_2(CN)_3$ at low temperature region is depicted in Figure 9b. The appearance of the superconducting state is interpreted by both the increase of W/U_{eff} and the deviation of t'/t from unity. The increase of T_c in the initial pressure regime might be ascribed to the reduction of the spin frustration. The following decrease of T_c in whole measured directions might be explained by the decrease of $D(\varepsilon_F)$ owing to the increase of W. The appearance of superconducting state immediately after the release of the spin frustration in the SL state is an indication of the importance of the magnetic mediation for SC.

10. OTHER SUPERCONDUCTORS INCLUDING SINGLE COMPONENT ONES

Besides ET, BO, TMTSF and TMTTF SCs, there are other SCs (Fig. 10, numbers in bracket are the total members of each SC and the

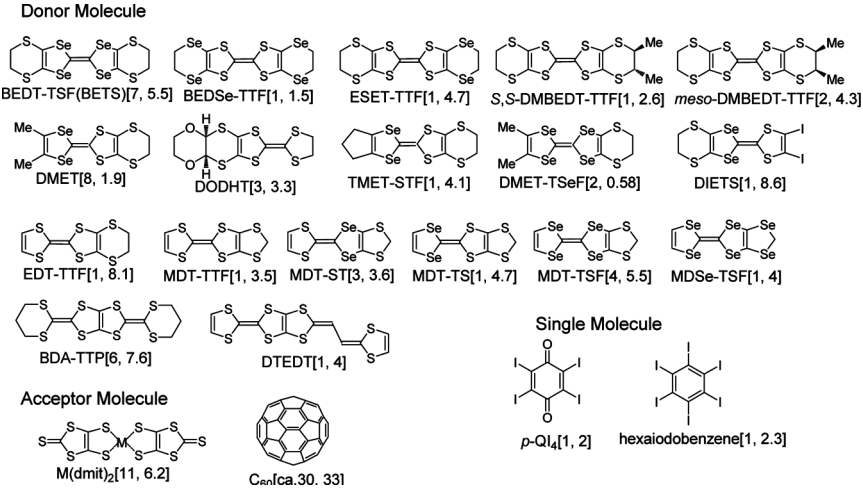

FIGURE 10 Component molecules of superconductors. The numbers in bracket indicate the total members of each superconductor and the highest T_c.

highest T_c) of CT salts based on symmetric (BETS [49], BEDSe-TTF [50]) and unsymmetric donors (ESET-TTF [51], *S*,*S*-DMBEDT-TTF [52], *meso*-DMBEDT-TTF [53], DMET [54], DODHT [55], TMET-STF [56], DMET-TSF [57], DIETS [58], EDT-TTF [59], MDT-TTF [60], MDT-ST [61], MDT-TS [62], MDT-TSF [63], MDSe-TSF [64], BDA-TTP [65], DTEDT [66]) as well as acceptors, $M(dmit)_2$ (M = Ni, Pd) [67] and C_{60} [68]. Most of the reported T_c's recently prepared are the on-set T_c values that are approximately 0.5–1 K higher than the mid-point T_c values. Except the last C_{60} system, the T_c's of them are less than 10 K. There are two single-component SCs, *p*-iodanil (*ca*. 2 K at 52 GPa) [69] and hexaiodobenzene (*ca*. 2.3 K at 58 GPa) [70]. At present the total numbers of molecular SCs are around 150 and the highest T_c is 33 K for $RbCs_2C_{60}$ [71].

11. UNIDENTIFIED SUPERCONDUCTING ORGANICS (USO)

There have been several experimental reports describing very high T_c's or very fascinating materials with low T_c though these data are not reproducible.

The most interesting one was Na salt of cholanate with $T_c = 277.0$ K reported in 1976, though cholanic acid does not have π-electrons [72]. The superconductivity was detected by conductivity and magnetic measurements. The authors mentioned that the salt showed an insulator to SC transition and the transition was fractional. Very recently,

biological compound (double stranded DNA) was reported to exhibit proximity induced superconductivity less than 1 K [73]. The deionized DNA molecules are insulating [74] and superconductivity cannot be expected.

In 1978, aniline black was reported to show possible superconductivity by the irreversible drop of resistivity by 10^6 in the *I-V* measurements at RT around 250 V ($T_c = 295.5$ K) [75]. In 1989, a resistance drop by nine orders of magnitude and a strong diamagnetism which was destroyed by magnetic field were reported on polypropylene oxidized for three years ($T_c = 293$ K) [76]. Oligo- and polyphthalocyanines have been reported to exhibit T_c of 83 and 92 K, detected by LFMA (low-field magnetic absorption) [77], which is very sensitive but sometimes gave false signal. Those are the USOs of polymers. So far no organic polymers have been confirmed to show superconductivity, although there are at least two inorganic ones (SN_x [78], black phosphorus [79]) with crystalline forms. It should be reminded that the sample should be well oriented otherwise disorders inherent to organic polymer destroy superconductivity.

As for the low molecular weight materials, Schön *et al*. reported superconductivity on polyacenes (anthracene, tetracene and pentacene) of FET devices at low temperatures ($T_c < 4$ K) but the paper was retracted [80].

REFERENCES

[1] Saito, G., Yamochi, H., Maesato, M., Yoshida, Y., Ota, A., & Shimizu, Y. (2004). Design of organic (super)conductors and study of their physical properties. In: *Organic Conductors, Superconductors and Magnets: From Synthesis to Molecular Electronics*, Ouahab, L. & Yagubskii, E. (Eds.), Kluwer Academic Pub.: Netherlands, 19–44.

[2] Ishiguro, T., Yamaji, K., & Saito, G. (1998). *Organic Superconductors*, 2nd Ed. Springer-Verlag: Berlin.

[3] Pac, S. & Saito, G. (2002). *J. Solid State Chem.*, *168*, 486–496.

[4] Horiuchi, S., Yamochi, H., Saito, G., Sakaguchi, K., & Kusunoki, M. (1996). *J. Am. Chem. Soc.*, *118*, 8604–8622.

[5] Saito, G., Sasaki, H., Aoki, T., Yoshida, Y., Otsuka, A., Yamochi, H., Drozdova, O., Yakushi, K., Kitagawa, H., & Mitani, T. (2002). *J. Mater. Chem.*, *12*, 1640–1649.

[6] (a) Ota, A., Yamochi, H., & Saito, G. (2002). *J. Mater. Chem.*, *12*, 2600–2602. (b) Chollet, M., Guerin, L., Uchida, N., Fukaya, S., Shimoda, H., Ishikawa, T., Matsuda, K., Hasegawa, T., Ota, A., Yamochi, H., Saito, G., Tazaki, R., Adachi, S., & Koshihara, S. (2005). *Science*, *307*, 86–89.

[7] Jerome, D. & Schulz, H. J. (1982). *Adv. Physics*, *31*, 299–490.

[8] Bechgaard, K. (1982). *Mol. Cryst. Liq. Cryst.*, *79*, 1–13.

[9] Sakata, M., Yoshida, Y., Maesato, M., Saito, G., Matsumoto, K., & Hagiwara, R. (2006). *Mol. Cryst. Liq. Cryst.*, *452*, 103–112.

[10] Balicas, L., Behnia, K., Kang, W., Canadell, E., Auban-Senzier, P., Jerome, D., Ribault, M., & Fabre, J. M. (1994). *J. Phys. I (France)*, *4*, 1539–1549.

[11] Adachi, T., Ojima, E., Kato, K., Kobayashi, H., Miyazaki, T., Tokumoto, M., & Kobayashi, A. (2000). *J. Am. Chem. Soc.*, *122*, 3238–3239.
[12] Auban-Senzier, P., Pasquier, C., Jerome, D., Carcel, C., Fabre, J. M. (2003). *Synth. Metals*, *133–134*, 11–14.
[13] Takigawa, M., Yasuoka, H., & Saito, G. (1987). *J. Phys. Soc. Jpn.*, *56*, 873–876.
[14] Jerome, D. (1991). *Science*, *252*, 1509–1514.
[15] Saito, G., Enoki, T., Toriumi, K., & Inokuchi, H. (1982). *Solid State Commun.*, *42*, 557–560.
[16] Beno, M. A., Wang, H. H., Kini, A. M., Carlson, K. D., Geiser, U., Kwok, W. K., Thompson, J. E., Williams, J. M., Ren, J., & Whangbo, M.-H. (1990). *Inorg. Chem.*, *29*, 1599–1601.
[17] Kahlich, S., Schweitzer, D., Heinen, I., Lan, S. E., Nuber, B., Keller, H. J., Winzer, K., & Helberg, H. W. (1991). *Solid State Commun.*, *80*, 191–195.
[18] Taniguchi, H., Miyashita, M., Uchiyama, K., Satoh, K., Mori, N., Okamoto, H., Miyagawa, K., Kanoda, K., Hedo, M., & Uwatoko, Y. (2003). *J. Phys. Soc. Jpn.*, *72*, 468–471.
[19] Schirber, J. E., Overmyer, D. L., Carlson, K. D., Williams, J. M., Kini, A. M., Wang, H. H., Charlier, H. A., Love, B. J., Watkins, D. M., & Yaconi, G. A. (1991). *Phys. Rev., B44*, 4666–4669.
[20] Saito, G., Yamochi, H., Nakamura, T., Komatsu, T., Inoue, T., Ito, H., Ishiguro, T., Kusunoki, M., Sakaguchi, K., & Mori, T. (1993). *Synth. Metals*, *55–57*, 2883–2890.
[21] Kini, M., Geiser, U., Wang, H. H., Carlson, K. D., Williams, J. M., Kwok, W. K., Vandervoort, K. G., Thompson, J. E., Stupka, D. L., Jung, D., & Wangbo, M.-H. (1990). *Inorg. Chem.*, *29*, 2555–2557.
[22] Urayama, H., Yamochi, H., Saito, G., Nozawa, K., Sugano, T., Kinoshita, M., Sato, S., Oshima, K., Kawamoto, A., & Tanaka, J. (1988). *Chem. Lett.*, *1988*, 55–58.
[23] Williams, J. M., Kini, A. M., Wang, H. H., Carlson, K. D., Geiser, U., Montgomery, L. K., Pyrka, G. J., Watkins, D. M., Kommers, J. M., Boryschuk, S. J., Crouch, A. V., Kwok, W. K., Schirber, J. E., Overmyer, D. L., Jung, D., & Whangbo, M.-H. (1990). *Inorg. Chem.*, *29*, 3272–3274.
[24] Ishiguro, T., Ito, H., Yamochi, Y., Ohmichi, E., Kubota, M., Yamochi, H., Saito, G., Kartsovnik, M. V., Tanatar, M. A., Sushko, Yu. V., & Logvenov, G. Yu. (1997). *Synth. Metals*, *85*, 1471–1478.
[25] Ito, H., Ishiguro, T., Kubota, M., & Saito, G. (1996). *J. Phys. Soc. Jpn.*, *65*, 2987–2993.
[26] Kanoda, K. (1997). *Hyperfine Interact.*, *104*, 235–249.
[27] Ito, H., Ishiguro, T., Kondo, T., & Saito, G. (2000). *J. Phys. Soc. Jpn.*, *69*, 290–291.
[28] Saito, G., Yamochi, H., Nakamura, T., Komatsu, T., Ishiguro, T., Nogami, Y., Ito, Y., Mori, H., Oshima, K., Nakashima, M., Uchida, S., Takagi, H., Kagoshima, S., & Osada, T. (1991). *Synth. Metals*, *41–43*, 1993–1998.
[29] Takahashi, T., Kanoda, K., & Saito, G. (1992). *Jpn. J. Appl. Phys.*, *7*, 414–418.
[30] Ichimura, K., Arai, T., Nomura, K., Takasaki, S., Yamada, J., Nakatsuji, S., & Anzai, H. (1997). *Physica C*, *282–287*, 1895–1896.
[31] Izawa, K., Yamaguchi, H., Sasaki, T., & Matsuda, Y. (2002). *Phys. Rev. Lett.*, *88*, 27002/1–4.
[32] Kini, A. M., Dudek, J. D., Carlson, K. D., Geiser, U., Klemm, R. A., Williams, J. M., Lykke, K. R., Schlueter, J. A., Wang, H. H., Wurz, P., Ferraro, J. R., Yaconi, G. A., & Stout, P. (1993). *Physica C*, *204*, 399–405.
[33] Toyota, N. (1996). *Physical Phenomena at High Magnetic Fields-II*. (World Sci.) 282–293.
[34] Komatsu, T., Matsukawa, N., Inoue, T., & Saito, G. (1996). *J. Phys. Soc. Jpn.*, *65*, 1340–1354.

[35] Drozdova, O., Saito, G., Yamochi, H., Okubo, K., Yakushi, K., Uruichi, M., & Ouahab, L. (2001). *Inorg. Chem.*, *40*, 3265–3266.
[36] Schirber, J. E., Venturini, E. L., Kini, A. M., Wang, H. H., Whitworth, J. R., & Williams, J. M. (1988). *Physica C*, *152*, 157–158.
[37] Schirber, J. E., Overmyer, D. L., Williams, J. M., Kini, A. M., & Wang, H. H. (1990). *Physica C*, *170*, 231–232.
[38] Schirber, J. E., Overmyer, D. L., Venturini, E. L., Wang, H. H., Carlson, K. D., Kwok, W. K., Kleinjan, S., & Williams, J. M. (1990). *Physica C*, *161*, 412–414.
[39] Parkin, S. S. P., Ribault, M., Jerome, D., & Bechgaard, K. (1981). *J. Phys. C14*, 5305–5326.
[40] Sparn, G., Thompson, J. D., Huang, S.-M., Kaner, R. B., Diederich, F., Whetten, R. L., Gruner, G., & Holczer, K. (1991). *Science*, *252*, 1829–1830.
[41] Kusuhara, H., Sakata, Y., Ueba, Y., Tada, K., Kaji, M., & Ishiguro, T. (1990). *Solid State Commun.*, *74*, 251–255.
[42] Tokumoto, M., Murata, K., Kinoshita, N., Yamaji, K., Anzai, H., Tanaka, Y., Hayakawa, Y., Nagasaka, K., & Sugawara, Y. (1990). *Mol. Cryst. Liq. Cryst.*, *181*, 295.
[43] Campos, C. E., Brooks, J. S., van Bentum, P. J. M., Perenboom, J. A. A., Rooks, J., Klepper, S. J., & Tokumoto, M. (1995). *Rev. Sci. Instrum.*, *66*, 1061–1064.
[44] (a) Mizutani, T., Tokumoto, M., Kinoshita, T., Brooks, J. S., Uwatoko, Y., Drozdova, O., Yakushi, K., Tamura, I., Kobayashi, H., Mangetsu, T., Yamada, J., & Ishida, K. (2003). *Synth. Metals*, *133–134*, 229–231.
(b) Ishikawa, T., Maesato, M., & Saito, G. (2003). *Synth. Metals*, *133–134*, 227–228.
(c) Ito, H., Hasegawa, Y., Ishihara, A., Takasaki, S., Yamada, J., & Anzai, H. (2003). *Synth. Metals*, *133–134*, 233–234.
[45] Maesato, M., Shimizu, Y., Ishikawa, T., Saito, G., Miyagawa, K., & Kanoda, K. (2004). *J. Phys. IV France*, *114*, 227–231.
[46] McKenzie, R. H. (1998). *Comments Condens. Matter Phys.*, *18*, 309–337.
[47] Kino, H. & Fukuyama, H. (1995). *J. Phys. Soc. Jpn.*, *64*, 2726–2729.
[48] Shimizu, Y., Miyagawa, K., Kanoda, K., Maesato, M., & Saito, G. (2003). *Phys. Rev. Lett.*, *91*, 107001/1–4.
[49] Kobayashi, H., Kobayashi, A., & Cassoux, P. (2000). *Chem. Soc. Rev.*, *29*, 325–333.
[50] Sakata, J., Sato, H., Miyazaki, A., Enoki, T., Okano, Y., & Kato, R. (1998). *Solid State Commun.*, *108*, 377–381.
[51] Okano, Y., Iso, M., Kashimura, Y., Yamaura, J., & Kato, R. (1999). *Synth. Metals*, *102*, 1703–1704.
[52] Zambounis, J. S., Mayer, C. W., Hauenstein, K., Hilti, B., Hofherr, W., Pfeiffer, J., Buerkle, M., & Rihs, G. (1992). *Adv. Mater.*, *4*, 33–35.
[53] Kimura, S., Maejima, T., Suzuki, H., Chiba, R., Mori, H., Kawamoto, T., Mori, T., Moriyama, H., Nishio, Y., & Kajita, K. (2004). *Chem. Commun.*, 2454–2455.
[54] Kikuchi, K., Murata, K., Honda, Y., Namiki, T., Saito, K., Ishiguro, T., Kobayashi, K., & Ikemoto, I. (1987). *J. Phys. Soc. Jpn.*, *56*, 3436–3439.
[55] Nishikawa, H., Morimoto, T., Kodama, T., Ikemoto, I., Kikuchi, K., Yamada, J., Yoshino, H., & Murata, K. (2002). *J. Am. Chem. Soc.*, *124*, 730–731.
[56] Kato, R., Yamamoto, K., Okano, Y., Tajima, H., & Sawa, H. (1997). *Chem. Commun.*, *1997*, 947–948.
[57] Kato, R., Aonuma, S., Okano, Y., Sawa, H., Tamura, M., Kinoshita, M., Oshima, K., Kobayashi, A., Bun, K., & Kobayashi, H. (1993). *Synth. Metals*, *61*, 199–206.
[58] Imakubo, T., Tajima, N., Tamura, M., Kato, R., Nishio, Y., & Kajita, K. (2002). *J. Mater. Chem.*, *12*, 159–161.

[59] Zhilyaeva, E. I., Torunova, S. A., Lyubovskaya, R. N., Mousdis, G. A., Papavassiliou, G. C., Perenboom, J. A. A. J., Pesotskii, S. I., & Lyubovskii, R. B. (2004). *Synth. Metals*, *140*, 151–154.
[60] Papavassiliou, G. C., Mousdis, G. A., Zambounis, J. S., Terzis, A., Hountas, A., Hilti, B., Mayer, C. W., & Pfeiffer, J. (1988). *Synth. Metals*, *B27*, 379–383.
[61] Takimiya, K., Takamori, A., Aso, Y., Otsubo, T., Kawamoto, T., & Mori, T. (2003). *Chem. Mater.*, *15*, 1225–1227.
[62] Takimiya, K., Kodani, M., Niihara, N., Aso, Y., Otsubo, T., Bando, Y., Kawamoto, T., & Mori, T. (2004). *Chem. Mater.*, *16*, 5120–5123.
[63] Takimiya, K., Kataoka, Y., Aso, Y., Otsubo, T., Fukuoka, H., & Yamanaka, S. (2001). *Angew. Chem. Int. Ed.*, *40*, 1122–1125.
[64] Kodani, M., Takamori, A., Takimiya, K., Aso, Y., & Otsubo, T. (2002). *J. Solid State Chem.*, *168*, 582–589.
[65] Yamada, J., Watanabe, M., Akutsu, H., Nakatsuji, S., Nishikawa, H., Ikemoto, I., & Kikuchi, K. (2001). *J. Am. Chem. Soc.*, *123*, 4174–4180.
[66] Misaki, Y., Higuchi, N., Fujiwara, H., Yamabe, T., Mori, T., Mori, H., & Tanaka, S. (1995). *Angew. Chem. Int. Ed. Engl.*, *34*, 1222–1225.
[67] Brossard, L., Ribault, M., Valade, L., & Cassoux, P. (1986). *Physica. B.*, *143*, 378–380.
[68] Hebard, A. F., Rosseinsky, M. J., Haddon, R. C., Murphy, D. W., Glarum, S. H., Palstra, T. T. M., Ramirez, A. P., & Kortan, A. R. (1991). *Nature*, *350*, 600–601.
[69] Yokota, T., Takeshita, N., Shimizu, K., Amaya, K., Onodera, A., Shirotani, I., & Endo, S. (1996). *Czech. J. Phys.*, Suppl. S2, *46*, 817–818.
[70] Iwasaki, E., Shimizu, K., Amaya, K., Nakayama, A., Aoki, K., & Carlon, R. P. (2001). *Synth. Metals*, *120*, 1003–1004.
[71] Tanigaki, K., Ebbesen, T. W., Saito, S., Mizuki, J., Tsai, J.-S., Kubo, Y., & Kuroshima, S. (1991). *Nature*, *352*, 222–223.
[72] Wolf, A. A. & Halpern, E. H. (1976). *Proceeding IEEE*, *64*, 357–359.
[73] Kasumov, A. Y., Kociak, M., Guéron, S., Reulet, B., Volkov, V. T., Klinov, D. V., & Bouchiat, H. (2001). *Science*, *291*, 280–282.
[74] Zhang, Y., Austin, R. H., Kraeft, J., Cox, E. C., & Ong, N. P. (2002). *Phys. Rev. Lett.*, *89*, 198102/1–4.
[75] Langer, J. (1978). *Solid State Commun.*, *26*, 839–844.
[76] Enikolopyan, N. S., Grigorov, L. N., & Smirnova, S. G. (1989). *JETP Lett.*, *49*, 371–375.
[77] (a) Lyubchenko, L. S., Stepanov, S. V., Lyubchenko, M. L., Sherle, A. I., Epstein, V. P., Dadali, A. A., & Malinsky, J. (1992). (Russia, USA), *Zhurnal Fizicheskoi Khimii*, *66*, 2510–2526.
(b) (1992). *Physics Letters A*, *162*, 69–78.
[78] (a) Greene, R. L., Street, G. B., & Suter, L. J. (1975). *Phys. Rev. Lett.*, *34*, 577–579.
(b) Labes, M. M., Love, P., & Nichols, L. F. (1979). *Chem. Rev.*, *79*, 1–15.
[79] Bridgman, P. W. (1916). *J. Am. Chem. Soc.*, *38*, 609–612.
[80] Schön, J. H., Kloc, Ch., & Batlogg, B. (2000). *Nature*, *406*, 702.